Self-powered active lateral suspension for railway vehicles

Wang, P, Mei, TX, Zhang, J and Li, H

http://dx.doi.org/10.1109/TVT.2015.2407575

This article has been accepted for publication in a future issue of this journal, but has not been fully edited. Content may change prior to final publication. Citation information: DOI 10.1109/TVT.2015.2407575, IEEE Transactions on Vehicular Technology

Self-powered Active Lateral Secondary Suspension for Railway Vehicles

Peng Wang, TX Mei, Jiye Zhang and Hong Li

***Abstract*—This paper presents a design methodology for the development of self-powered active lateral secondary suspensions for rail vehicles. It firstly investigates the energy flows in the active lateral secondary suspensions and analyzes the conditions for self-powered control in detail. The impact of the controller design on both the ride quality and the energy consumption is then used to guide the design/specification of actuators and to define key actuator parameters in order to achieve both expected performance improvement and zero-energy consumption for the actuators. Furthermore, a control strategy for dealing with larger than expected energy consumptions by the active suspensions is proposed to eliminate excessive power requirements, but also to ensure the ride quality improvement in comparison to that of passive suspensions. Computer simulations are used to validate the control strategy for the self-powered active suspension.**

***Index Terms*—active suspension, energy consumption, optimal control, railway vehicles, self-powered suspension.**

I. Introduction

Active suspensions have been shown to greatly improve the passenger comfort in both road and railway vehicles in comparison to the conventional passive suspensions. The improvement in performance is possible because of the ability of actuators to both absorb and supply energy. However external energy supplies are normally required to power the active suspensions, which is one of the main drawbacks of an active vibration control system. To overcome the problem, there have recently been studies into the concept of self-powered active suspensions. Suda and Shiiba [1] proposed an energy-regenerative suspension by using a rotary DC-motor with a rack-pinion mechanism as the actuator. Nakano K, etc. [2],[3] studied a novel configuration for the energy regeneration system with the use of two DC-motors where one motor is used to absorb the kinetic energy and the other to provide improved damping, although it is also possible to use a single motor in both motoring and generative modes as presented in [4],[5]. Also, Zuo [6],[7] studied how the vehicle performance and the energy harvesting may be influenced by factors such as road roughness, vehicle speed and suspension/tire parameters. Whilst those studies have shown the feasibility and general principle of self-powered active suspensions for road vehicles, there is no consideration for rail specific issues and also little has been reported on the general design approach of the self-powered active suspensions to optimize the vehicle performance. With the development of high-speed railway, the increased speed can lead to significantly increased body vibrations of railway vehicles and there is an increased demand for the use of the active technologies. Although active controls have been studied for many years [8][9], some further progress on the secondary lateral suspensions has been reported recently. Anneli applied a hold-off-device [10] to improve the ride quality in curves and investigated the performance of a H∞ control strategy for the lateral vibration damping for railway vehicles [11]. Zhou, etc. [12] presented a novel suspension by integrating tilting control with active lateral secondary suspensions which can provide both good ride comfort and effective tilt. However, no self-powered concept for active suspensions of rail vehicles was considered in previous studies [8]-[12], even though some energy consumption analysis was provided in [13][14]. Therefore this paper investigates in detail the energy consumption and regeneration in the lateral secondary active suspensions for railway vehicles and proposes a new design methodology to optimize the self-powered active suspensions where the improvement on the ride quality is maximized within the constraint of the kinetic energy harvested from the vibrations. In the proposed design approach, the detailed analysis of the power balance conditions based on real track misalignment data is used to develop the actively controlled suspensions for desired performance improvements and also to help with the design/specification of actuators that will meet the self-powering requirement.

Manuscript received May 15, 2014; date of current version February 24, 2015. This work was supported in part by National Natural Science Foundation of China (11172247, 11402214).

P. Wang and J.Y. Zhang are with the Transaction Power State Key Laboratory, Southwest Jiaotong University, Chengdu 610031, China (e-mail: ertongtuanyuan@163.com; jyzhang@swjtu.edu.cn).

TX Mei is with School of Computer, Science and Engineering, University of Salford, Manchester, M5 4WT, UK (t.x.mei@salford.ac.uk).

H. Li is with the Department of Engineering and Technology, Manchester Metropolitan University, M1 5GD Manchester, UK (email: hong.li@ mmu .ac.uk).

II. Analytical Model

A. The Overall System and Analytical Model

Fig.1 shows a block diagram of the overall control system. A conventional railway passenger vehicle is used in the study, which consists of two bogies and four wheelsets. The vehicle is controlled at the front and rear by two electro-mechanical actuator units, each with an independent DC/DC converter controlling the voltage supplied from the power storage (batteries or super capacitors). The force applied by each

This article has been accepted for publication in a future issue of this journal, but has not been fully edited. Content may change prior to final publication. Citation information: DOI 10.1109/TVT.2015.2407575, IEEE Transactions on Vehicular Technology

actuator to the vehicle body is controlled by an internal 'force controller'. The force demand for the two actuators is produced by the 'active controller' which acts upon the sensor measurements from the vehicle. The electrical machines used in the actuators will be capable of operating in both motoring and regenerating modes. The control objective of this study is to provide a performance improvement for a mechanical object (i.e. the vehicle), but through the use of sensors, control electronics and electric actuators without the need for additional power supply.

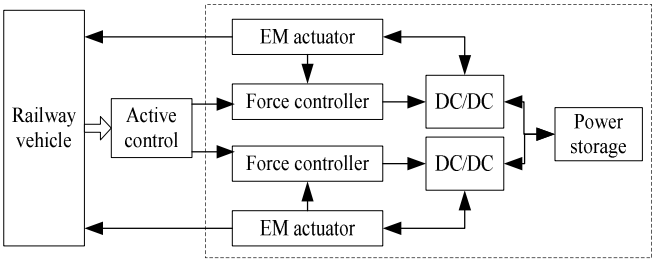

Fig.1. The overall control system

This paper will be focused on the theoretical development and optimization of the control design method for the self-powered concept, in particular a detailed analysis of the power balance condition and its impact on the design of the actuators and control laws. The simulation models including the vehicle dynamics, the actuators and associated controls are used to validate the findings. A further work is planned to develop a hardware-in-the-loop platform to demonstrate the full potential of the self-powered active suspensions for rail vehicles, the outcome of which will be published separately. The vehicle dynamics will still be represented by a simulation model, but the self contained actuators and the active controller will be implemented with physical hardware. Two extra actuators and two load cells will be installed to interact with the existing actuators and will be controlled to follow the vehicle motions computed from the simulation model in real time. The output of the load cells will represent the control forces applied to the vehicle by the actuators, whereas the feedback measurement from the vehicle will be produced from the simulation results in real time and fed to the active control via D/A converters.

B. Vehicle Dynamics

The end view diagram of the railway vehicle is shown in Fig.2, where the parameters are listed in Appendix TABLE V. All motions related to the lateral dynamics of the vehicle are included in the model for the study (i.e. the lateral, yaw and roll motions) and the governing equations of the vehicle dynamics are given in equations (1)-(8) [15].

1) Wheelset dynamics (i=1~2 while j=1, i=3~4 while j=2)

$$M_w\ddot{y}_{wi}=K_{py}[y_{tj}-(-1)^i a\psi_{tj}-h_{tp}\theta_{tj}-y_{wi}]+C_{py}[\dot{y}_{tj}-(-1)^i a\dot{\psi}_{tj}-h_{tp}\dot{\theta}_{tj}-\dot{y}_{wi}]-\frac{2f_{22}}{V}\dot{y}_{wi}+2f_{22}\psi_{wi} \quad (1)$$

$$I_{wz}\ddot{\psi}_{wi}=K_{px}b_1^2(\psi_{tj}-\psi_{wi})+C_{px}b_1^2(\dot{\psi}_{tj}-\dot{\psi}_{wi})-\frac{2f_{11}b^2}{V}\dot{\psi}_{wi}-\frac{2f_{11}\lambda b}{r_0}(y_{wi}-y_{ri}) \quad (2)$$

2) Bogie dynamics (i=1~2)

$$\begin{aligned}M_t\ddot{y}_{ti}&=K_{sy}[y_c-(-1)^i l\psi_c-h_{cs}\theta_c-h_{ts}\theta_{ti}-y_{ti}]-U_i\\&-K_{py}(y_{ti}+a\psi_{ti}-h_{tp}\theta_{ti}-y_{w,2i-1})-C_{py}(\dot{y}_{ti}+a\dot{\psi}_{ti}-h_{tp}\dot{\theta}_{ti}-\dot{y}_{w,2i-1})\\&-K_{py}(y_{ti}-a\psi_{ti}-h_{tp}\theta_{ti}-y_{w,2i})-C_{py}(\dot{y}_{ti}-a\dot{\psi}_{ti}-h_{tp}\dot{\theta}_{ti}-\dot{y}_{w,2i}) \quad (3)\end{aligned}$$

$$\begin{aligned}I_{tz}\ddot{\psi}_{ti}&=K_{sx}b_2^2(\psi_c-\psi_{ti})+C_{sx}b_2^2(\dot{\psi}_c-\dot{\psi}_{ti})\\&-K_{py}a(y_{ti}+a\psi_{ti}-h_{tp}\theta_{ti}-y_{w,2i-1})-C_{py}a(\dot{y}_{ti}+a\dot{\psi}_{ti}-h_{tp}\dot{\theta}_{ti}-\dot{y}_{w,2i-1})\\&+K_{py}a(y_{ti}-a\psi_{ti}-h_{tp}\theta_{ti}-y_{w,2i})+C_{py}a(\dot{y}_{ti}-a\dot{\psi}_{ti}-h_{tp}\dot{\theta}_{ti}-\dot{y}_{w,2i})\\&-K_{px}b_1^2(\psi_{ti}-\psi_{w,2i-1})-C_{px}b_1^2(\dot{\psi}_{ti}-\dot{\psi}_{w,2i-1})\\&-K_{px}b_1^2(\psi_{ti}-\psi_{w,2i})-C_{px}b_1^2(\dot{\psi}_{ti}-\dot{\psi}_{w,2i}) \quad (4)\end{aligned}$$

$$\begin{aligned}I_{tx}\ddot{\theta}_{ti}&=K_{sy}h_{ts}[y_c-(-1)^i l\psi_c-h_{cs}\theta_c-h_{ts}\theta_{ti}-y_{ti}]-U_i h_{ts}\\&+K_{sz}b_4^2(\theta_c-\theta_{ti})+C_{sz}b_4^2(\dot{\theta}_c-\dot{\theta}_{ti})+K_{py}h_{tp}(y_{ti}+a\psi_{ti}-h_{tp}\theta_{ti}-y_{w,2i-1})\\&+C_{py}h_{tp}(\dot{y}_{ti}+a\dot{\psi}_{ti}-h_{tp}\dot{\theta}_{ti}-\dot{y}_{w,2i-1})+K_{py}h_{tp}(y_{ti}-a\psi_{ti}-h_{tp}\theta_{ti}-y_{w,2i})\\&+C_{py}h_{tp}(\dot{y}_{ti}-a\dot{\psi}_{ti}-h_{tp}\dot{\theta}_{ti}-\dot{y}_{w,2i})-2K_{pz}b_3^2\theta_{ti}-2C_{pz}b_3^2\dot{\theta}_{ti} \quad (5)\end{aligned}$$

3) Car body dynamics

$$\begin{aligned}M_c\ddot{y}_c&=-K_{sy}(y_c+l\psi_c-h_{cs}\theta_c-h_{ts}\theta_{t1}-y_{t1})\\&-K_{sy}(y_c-l\psi_c-h_{cs}\theta_c-h_{ts}\theta_{t2}-y_{t2})+U_1+U_2 \quad (6)\end{aligned}$$

$$\begin{aligned}I_{cz}\ddot{\psi}_c&=-K_{sy}l(y_c+l\psi_c-h_{cs}\theta_c-h_{ts}\theta_{t1}-y_{t1})-K_{sx}b_2^2(\psi_c-\psi_{t1})\\&+K_{sy}l(y_c-l\psi_c-h_{cs}\theta_c-h_{ts}\theta_{t2}-y_{t2})-C_{sx}b_2^2(\dot{\psi}_c-\dot{\psi}_{t1})\\&-K_{sx}b_2^2(\psi_c-\psi_{t2})-C_{sx}b_2^2(\dot{\psi}_c-\dot{\psi}_{t2})+(U_1-U_2)l \quad (7)\end{aligned}$$

$$\begin{aligned}I_{cx}\ddot{\theta}_c&=K_{sy}h_{cs}(y_c+l\psi_c-h_{cs}\theta_c-h_{ts}\theta_{t1}-y_{t1})-K_{sz}b_4^2(\theta_c-\theta_{t1})\\&+K_{sy}h_{cs}(y_c-l\psi_c-h_{cs}\theta_c-h_{ts}\theta_{t2}-y_{t2})-C_{sz}b_4^2(\dot{\theta}_c-\dot{\theta}_{t1})\\&-K_{sz}b_4^2(\theta_c-\theta_{t2})-C_{sz}b_4^2(\dot{\theta}_c-\dot{\theta}_{t2})-(U_1+U_2)h_{cs} \quad (8)\end{aligned}$$

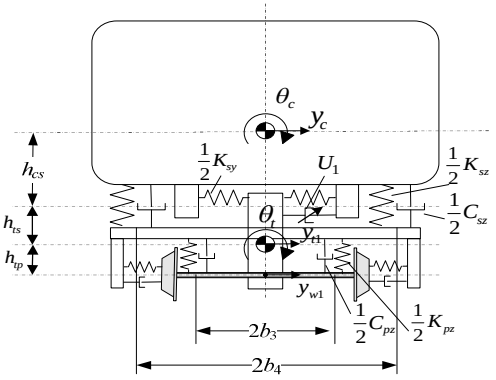

Fig.2. The end view diagram of the railway vehicle.

Note that, in the study, the passive dampers are replaced by the actuators for the study of actively controlled suspensions and the actuator forces are the control input. For the simulation of the passive vehicle in the comparative assessment, the actuator forces in the model are replaced by the damping forces of the passive dampers (C_{sy}). The vehicle model (1)-(8) can be represented in the state-space form as shown in (9).

$$\dot{\boldsymbol{x}}=\boldsymbol{A}\boldsymbol{x}+\boldsymbol{B}\boldsymbol{u}+\boldsymbol{F}\boldsymbol{w} \quad (9)$$

where $\boldsymbol{x}=[\boldsymbol{q},\dot{\boldsymbol{q}}]^T$, $\boldsymbol{q}=[y_c,\psi_c,\theta_c,y_{t1},\psi_{t1},\theta_{t1},y_{t2},\psi_{t2},\theta_{t2},y_{w1},\psi_{w1},y_{w2},\psi_{w2},y_{w3},\psi_{w3},y_{w4},\psi_{w4}]^T$,

$$\boldsymbol{A}=\begin{bmatrix}0 & \boldsymbol{I}\\ \boldsymbol{S}_2^{-1}\boldsymbol{S}_0 & \boldsymbol{S}_2^{-1}\boldsymbol{S}_1\end{bmatrix},\ \boldsymbol{B}=\begin{bmatrix}0\\ \boldsymbol{S}_2^{-1}\boldsymbol{S}_u\end{bmatrix},\ \boldsymbol{F}=\begin{bmatrix}0\\ \boldsymbol{S}_2^{-1}\boldsymbol{S}_w\end{bmatrix}.$$

This article has been accepted for publication in a future issue of this journal, but has not been fully edited. Content may change prior to final publication. Citation information: DOI 10.1109/TVT.2015.2407575, IEEE Transactions on Vehicular Technology

$\boldsymbol{S}_2, \boldsymbol{S}_1$ and $\boldsymbol{S}_0$ are the mass, damping and stiffness matrixes. $\boldsymbol{u}=[U_1,U_2]^T$ is the control input vector. $\boldsymbol{w}=[y_{r1},y_{r2},y_{r3},y_{r4}]^T$ represents the track irregularities. $\boldsymbol{S}_u$ and $\boldsymbol{S}_w$ are the corresponding coefficient matrixes related to $\boldsymbol{u}$ and $\boldsymbol{w}$.

C. Active Controller

A number of control strategies have been proposed in the past for the active suspensions, including the classical sky-hook control and model based control methods [8]-[14]. The LQR control approach is used in this study, but the general principle and findings (from the energy consumption and harvesting analysis) will be similarly applicable for tuning and optimizing other strategies. The performance index of the LQR controller is chosen as

$$J=\lim_{T\to\infty}\frac{1}{T}\int_0^T\left[\rho_1\ddot{y}_c^2+\rho_2\ddot{\psi}_c^2+\rho_3\ddot{\theta}_c^2+\rho_4\left(U_1^2+U_2^2\right)\right]dt \quad (10)$$

where $\rho_1,\rho_2,\rho_3,\rho_4$ are the weighting factors for the ride comfort measures (lateral, yaw and roll accelerations of the vehicle body) and the control effort. The weighted output vector is

$$\boldsymbol{y}=[\ddot{y}_c,\ddot{\psi}_c,\ddot{\theta}_c]^T=\boldsymbol{C}\boldsymbol{x}+\boldsymbol{D}\boldsymbol{u} \quad (11)$$

where $\boldsymbol{C}$ and $\boldsymbol{D}$ can be readily formed using corresponding rows of $\boldsymbol{A}$ and $\boldsymbol{B}$. The performance index can be rewritten as

$$J=\lim_{T\to\infty}\frac{1}{T}\int_0^T\left(\boldsymbol{y}^T\boldsymbol{Q}_1\boldsymbol{y}+\boldsymbol{u}^T\boldsymbol{R}_1\boldsymbol{u}\right)dt \quad (12)$$

where $\boldsymbol{Q}_1=\mathrm{diag}(\rho_1,\rho_2,\rho_3)$, $\boldsymbol{R}_1=\mathrm{diag}(\rho_4,\rho_4)$. Let $\boldsymbol{Q}=\boldsymbol{C}^T\boldsymbol{Q}_1\boldsymbol{C}$, $\boldsymbol{R}=\boldsymbol{D}^T\boldsymbol{Q}_1\boldsymbol{D}+\boldsymbol{R}_1$, $\boldsymbol{N}=\boldsymbol{C}^T\boldsymbol{Q}_1\boldsymbol{D}$, weighting matrixes $\boldsymbol{Q}$, $\boldsymbol{R}$ and $\boldsymbol{N}$ are derived from the performance index (12) by using (11). A full state feedback controller may be obtained by applying the MATLAB command '$\boldsymbol{K}$=lqr($\boldsymbol{A}$,$\boldsymbol{B}$,$\boldsymbol{Q}$,$\boldsymbol{R}$,$\boldsymbol{N}$)'

$$\boldsymbol{u}=\boldsymbol{K}\boldsymbol{x} \quad (13)$$

The tuning of the weighting factors in the design of the control gain matrix in the next section will be mainly focused on the energy balance conditions, but attention is also given to ensure the maximum deflections of the both secondary and primary suspensions do not exceed their expected ranges of travel which are set at 60mm and 10mm respectively in the study.

III. Primary Analysis of Energy Consumption

This section is to establish a fundamental understanding of energy flows and its relationship with the suspension performance. Therefore, the technical detail of the actuator is not considered at this stage.

A. Calculation of Energy Consumption

The power of the two actuators P_1, P_2, can be calculated using (14).

$$\begin{cases}P_1=U_1\cdot\dot{z}_1+\eta\cdot\left|U_1\cdot\dot{z}_1\right|\\ P_2=U_2\cdot\dot{z}_2+\eta\cdot\left|U_2\cdot\dot{z}_2\right|\end{cases} \quad (14)$$

where $\dot{z}_1,\dot{z}_2$ denote the lateral velocities of the actuators at the front and the rear bogies and the coefficient $0\le\eta<100\%$ represents the internal power loss of the actuators.

Two different modes of operation for the actuators are considered: 1) Drive mode: if $P_1>0$, the actuator utilizes the energy from power source; and 2) Regeneration mode: if $P_1<0$, the actuator receives the energy from the suspension and stores it to the power source. The recoverable power is restricted as $(1-\mu)\cdot P_1$, where the coefficient $0\le\mu\le100\%$ represents the losses of the power source to store the recovered energy. The energy consumed by the actuators may be computed by integrating the power and a negative value indicates that the energy is being generated from the suspensions.

B. Trade-off between Ride Quality and Energy Consumption

For the self-powered suspensions, a trade-off between the ride quality improvement and the energy balance must be considered. In the analysis, the power losses of the actuators and the power source are initially set as $\eta=35\%$ and $\mu=0\%$ respectively, and the average ($\ddot{y}_{ca}$) of the lateral accelerations of the car body at the center of the vehicle ($\ddot{y}_c$) and above the front ($\ddot{y}_{c1}$) and rear ($\ddot{y}_{c2}$) bogies is used as the ride quality indicator. For practical relevance, the lateral track irregularities of measured data from three different track sections between Paddington and Bristol stations in the UK are used in the simulations as the track input. The key characteristics of the track sections are given in TABLE I. Track section 1 is the smoothest section and section 3 is the roughest section, while section 2 includes both smooth and rough parts.

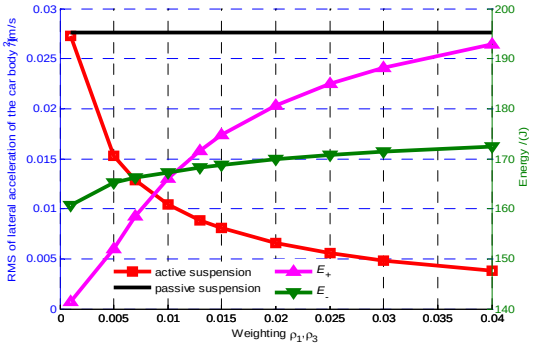

(a)

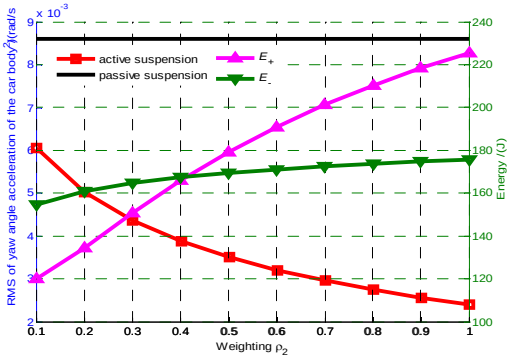

(b)

Fig.3. The impact of the weightings $\rho_1,\rho_2,\rho_3,\rho_4$ on the ride quality and the energy consumption. (a) RMS of $\ddot{y}_c$ and energy consumption when $\rho_1=\rho_3\in[0.005,0.04]$, $\rho_2=0.4$, $\rho_4=4.0\times10^{-11}$. (b) RMS of $\ddot{\psi}_c$ and energy consumption when $\rho_2\in[0.1,1]$, $\rho_1=\rho_3=0.01$, $\rho_4=4.0\times10^{-11}$.

In the control design, the effect of each of the weighting factors on the ride quality improvement and the energy consumption is studied. There is however a strong interaction between the lateral and roll motions of the vehicle body ($\ddot{y}_c$ and $\ddot{\theta}_c$) and therefore ρ_1 and ρ_3 may be considered together,

This article has been accepted for publication in a future issue of this journal, but has not been fully edited. Content may change prior to final publication. Citation information: DOI 10.1109/TVT.2015.2407575, IEEE Transactions on Vehicular Technology

whereas the yaw motion ($\ddot{\psi}_c$) affects mainly the lateral accelerations at the front and rear sections of the body so that ρ_2 needs to be tuned independently. The relationships between the weightings and the energy consumption (computed using the irregularity data of the track section 1) are revealed in Fig.3, where results for the passive suspension are also provided for comparison.

In Fig.3, E+ and E- are used to represent the positive and the negative energy consumption for the active suspensions. It can be seen that, at ρ_1, ρ_3 of 0.012 and ρ_2 of 0.42, the positive energy consumption equal to the negative one, indicating that the self-powered condition is possible for the weighting below those values. On the other hand, the value of ρ_1, ρ_3 should be greater than 0.005 and ρ_2 than 0.2 in order to deliver a ride quality much better than that of the passive suspension. The same process of the analysis is carried out for the weighting ρ_4, resulting in a value between 2×10^{-11} and 4×10^{-11} to meet the two design objectives.

Based on the analysis, the weightings $\rho_1 = 0.01$, $\rho_2 = 0.4$, $\rho_3 = 0.01$ and $\rho_4 = 4\times10^{-11}$ are selected and applied to all three sections of the track. The results are given in TABLE I. There is clearly substantial improvement in the reduction of the body acceleration by the active suspension in comparison with the passive vehicle in all three track conditions. When the control law is designed based on the smoothest section (track section 1), the energy balance is also achieved for the other two sections possibly because there is more kinetic energy available for harvesting.

C. *Primary Analysis on Energy Balance Condition*

As the losses in the actuators and the power storage (η, μ represent the percentage of each loss, respectively) are two main practical constraints for the effective self-powered operation of the active suspensions, a detailed study using different values of η (5-50%) and μ (0-50%) is carried out. The simulation results of the energy consumption using track section 1 as input are presented in Fig.4, where the same control gains as above are applied.

Fig.4 shows that when the power loss of the energy recovery/storage is above 50%, the active suspension cannot achieve the self-powered condition even if the internal power losses of the actuator are low. However, if $\mu \le 50\%$, a reasonable value of η can be found to satisfy the requirement of energy balance. Also, there seems to be a limit on the value of η (35% in the study) beyond which the energy balance requirement is not achievable even if μ = 0%. In order to validate the conclusions from Fig.4, simulation results on all 3 track sections are produced and given in TABLE II where μ is fixed at 10% and η is set at different values.

TABLE II indicates that it is easier to achieve a self-powered control on a higher level of track roughness where the requirement for the efficiency of the actuator and the power recovery is lower. Hence it is necessary to design such suspension systems using the relatively smooth track input, so that the energy balance can also be achieved for other sections with rougher irregularities.

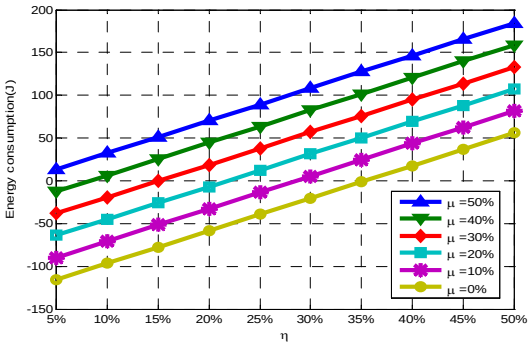

Fig.4. The relationship among η, μ and energy consumption

TABLE II
STATISTICS OF ENERGY CONSUMPTION WITH DEFFIERENT η

Track No.	$\eta = 25\%$ W(J)	$\eta = 28.5\%$ W(J)	$\eta = 31.5\%$ W(J)	$\eta = 32.5\%$ W(J)	$\eta = 35\%$ W(J)
1	-13.60	-0.29	10.93	14.92	24.43
2	-148.87	-68.40	-0.57	23.57	81.05
3	-126.01	-67.46	-18.12	-0.55	41.27

IV. ACTUATOR MODELING AND OUTLINE DESIGN

The analysis of the energy consumption in the last section is a primary analysis based on the estimation results using η and μ. However, it is necessary to understand the energy flows in the system by including a detailed actuator model to further analyze the energy balance conditions.

A. *Model of the Actuator*

In this study, the electro-mechanical actuation [14] is considered in order to meet the main requirement for the self-powered active suspension for railway vehicles, e.g. achievable force bandwidth, stroke, availability of power source, reliability, maintainability and costs. The structure of the actuator is presented in Fig.5

The actuator is composed of two main parts: a DC motor and a ball-screw mechanism set. The motor produces the required torque and the ball-screw set converts the rotation of the motor to the linear motion to provide a required force that acts between the car body and the bogie. An equivalent model of the actuator is also presented in Fig.5. The connection

TABLE I
STATISTICS OF RIDE QUALITY INDEXES AND ENERGY CONSUMPTION

Track No.	Lateral irregularities			Passive suspension			Active suspension			
	Max (mm)	RMS (mm)	Length (km)	RMS of $\ddot{y}_{ca}$ (mm/s^2)	RMS of $\ddot{\psi}_c$ (mrad/s^2)	RMS of $\ddot{\theta}_c$ (mrad/s^2)	RMS of $\ddot{y}_{ca}$ (mm/s^2)	RMS of $\ddot{\psi}_c$ (mrad/s^2)	RMS of $\ddot{\theta}_c$ (mrad/s^2)	Energy W(J)
1	3.7	1.0	2.5	64.0	8.6	12.2	27.8	3.9	5.5	−1.3
2	13.4	1.5	6.0	99.2	13.5	18.8	44.3	6.2	8.8	−78.0
3	12.8	3.2	1.0	199.0	27.2	37.8	90.1	12.3	18.2	−75.4

This article has been accepted for publication in a future issue of this journal, but has not been fully edited. Content may change prior to final publication. Citation information: DOI 10.1109/TVT.2015.2407575, IEEE Transactions on Vehicular Technology

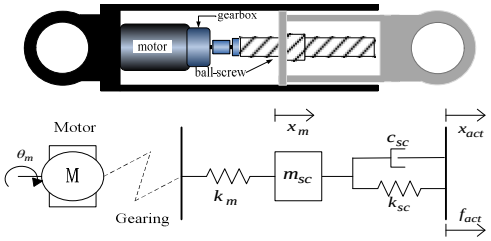

Fig.5. Ball-screw electro-mechanical actuator.

between the actuator and the vehicle is represented by the springs k_m, k_{sc}, whereas the damper c_{sc} represents the material damping effect in the connection. The model for the actuator is

$$\begin{cases} \dot{i}_a = -\dfrac{r_{arm}}{l_{arm}} i_a - \dfrac{k_e}{l_{arm}} \dot{\theta}_m + \dfrac{1}{l_{arm}} v_a \\ \ddot{\theta}_m = \dfrac{k_t}{J_m} i_a - \dfrac{c_m}{J_m} \dot{\theta}_m - \dfrac{k_m n^2}{J_m} \theta_m + \dfrac{k_m n}{J_m} x_m \\ \ddot{x}_m = \dfrac{k_m n}{m_{sc}} \theta_m - \dfrac{k_m + k_{sc}}{m_{sc}} x_m - \dfrac{c_{sc}}{m_{sc}} \dot{x}_m + \dfrac{k_{sc}}{m_{sc}} x_{act} + \dfrac{c_{sc}}{m_{sc}} \dot{x}_{act} \\ f_{act} = k_{sc} x_m + c_{sc} \dot{x}_m - k_{sc} x_{act} - c_{sc} \dot{x}_{act} \end{cases} \quad (15)$$

The definitions of symbols of the actuator are listed in Appendix TABLE VI and the selection of the key parameters is explained in the following part.

B. Outline design of the Actuator

The parameters and dynamic response of the actuators will not only affect the performance of the active suspensions, but also can have substantial impact on the energy consumed. So the following analysis is to investigate suitable selection of the parameters to realize the self-powered active suspension. The total energy consumed or harvested by the actuator, should be at least equal to that generated by the suspension if the loss in the power conversion is negligible. To construct the relationship between the actuator's parameters and power consumption, it is assumed that the output torque of the motor can be converted to the output force of the actuator with high efficiency and the velocity of the actuator is almost equal to the stroke speed of the motor according to [5], i.e.

$$\begin{cases} n \cdot f_{act} \approx k_t i_a \\ \dot{x}_{act} \approx \dot{x}_m = n \cdot \dot{\theta}_m \end{cases} \quad (16)$$

From (15) and (16), the power consumption can be given by (17), where the storage/release of the energy of the motor inductance is excluded.

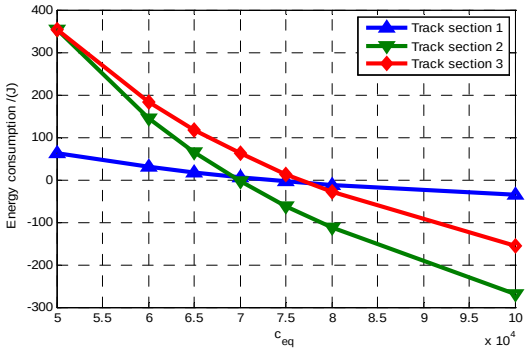

Fig.6. The relationship between c_{eq} and energy consumption

$$P_a = v_a \cdot i_a \approx (1/c_{eq}) \cdot f_{act}^2 + \dot{x}_{act} \cdot f_{act} \quad (17)$$

where $c_{eq} = (1/r_{arm}) \cdot (k_t / n)^2$.

The coefficient c_{eq} represents the internal power loss of the actuator and hence will have to be included in the analysis of the energy balance condition. Fig. 6 shows the energy consumption of the actuators with different values of c_{eq} on the 3 different sections of the track data. It is clear from the figure that a larger value of c_{eq} will lead to a higher level of energy for harvesting. To satisfy the self-powered requirement, the energy consumption needs to be zero or negative, i.e. c_{eq} >7.65x10^4.

Also other working conditions of the actuator, including the maximum suspension deflection, speed, average and peak force, are considered using simulation results from Section III. After assuming a maximum motor speed of 3000 rpm, the screw pitch is determined as 7.71×10^{-4} and the rated torque and the maximum torque of the motor are obtained as 0.93Nm and 3.58Nm, respectively. The main parameters for the motor and the ball-screw as determined are listed in TABLE VI. A motor and a ball-screw are consequently selected from a Baldor catalogue for a DC servo motor and an SKF catalogue for a SX/BX universal screw to meet the requirements. For the performance assessment and further energy analysis, the vehicle model is integrated in the simulation with the model of the actuator where a proportional and integral (PI) controller is used for a high bandwidth control of the actuators to deliver the desired actuator forces.

V. Further Energy Analysis

A. Energy comparison between actuator model and η

In section III, the coefficient η is used to simplify the representation of the energy loss in the actuator in order to enable the analytical study of the power flows and energy balance conditions without the need to include the complex actuator dynamics. The appropriateness of this simplified approach can be demonstrated by a close match between approximated energy consumption estimated using the simple coefficient representation and results produced using the full vehicle and actuator model, as shown in Fig.7.

Fig.7 indicates that the internal power loss of the actuator represents different proportions of the actuator's output power on different track situations, with the value of η at 28%, 31.5% and 33% for different track situations. Despite the small differences, it seems reasonable to use an average value of η to evaluate the power consumption and to design the optimal control law without having to include the detailed actuator dynamics in the design process as presented in the previous analysis in Section III. Also it is clear that the track section 1 represents the worst case in comparison to the other two track sections and that the energy balance condition derived using track section 1 is applicable to other two sections where the energy consumptions are largely negative and actuators work with a higher level of efficiency in terms of energy usage.

B. Control Strategy

It should be noted that the efficiency of the power source is

This article has been accepted for publication in a future issue of this journal, but has not been fully edited. Content may change prior to final publication. Citation information: DOI 10.1109/TVT.2015.2407575, IEEE Transactions on Vehicular Technology

not considered when designing the actuator in Section IV. If the chosen parameters are not sufficient to provide extra margins for energy consumption, the selected actuator may only achieve energy balance when there is low power loss in the power source (for energy storage). According to Fig. 4, the energy loss in the power source μ should be less than 5% as η is around 33% for the selected actuator in this study. In the case of additional energy loss or (unexpected) changes in track conditions where the energy balance condition can no longer be met, there is a need to maintain the basic operation of the self-powered active suspensions by switching to a control setting that is less demanding on power consumption but still able to maintain the ride comfort improvement as much as possible. Therefore a revised control strategy is proposed as given below.

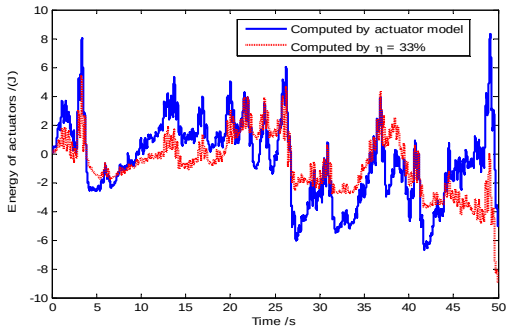

(a)

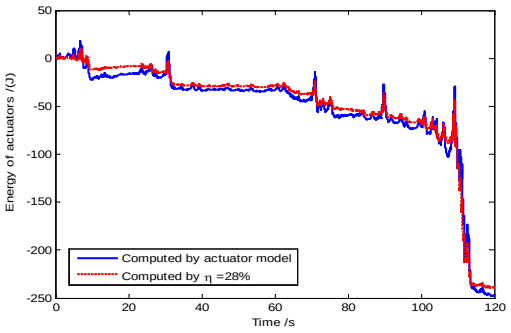

(b)

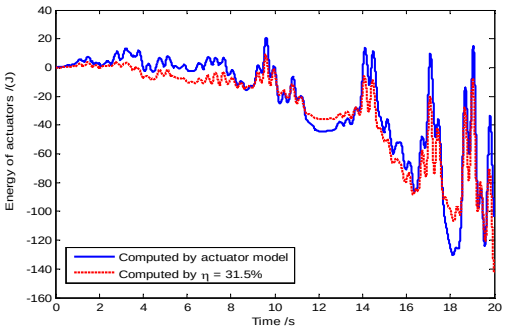

(c)

Fig. 7. Approximation of energy consumption by using η .(a) Track section 1. (b) Track section 2. (c) Track section 3.

It is reasonable to assume that there is sufficient initial energy stored in the power source (E_{ini} < 0) which will not be exhausted in the designed condition – this is possible, because the energy may be harvested as the vehicle accelerates or travels at lower speeds where the ride quality is not an issue and hence the active suspension can be used primarily to charge up the power supply.

When the energy storage (W) is above a predefined threshold (E_{th}), the controller gain ($\boldsymbol{K_o}$) will be used to provide the best ride quality under the self-energy sufficient condition. However, in the case where there is an unexpected reduction in the level of energy recovered and the energy storage falls below the threshold, the controller will be switched to use a lower gain ($\boldsymbol{K_p}$) that will provide a reduced performance of the ride quality (but no worse than what a conventional passive suspension would deliver). This process of switching can obviously reverse if the energy storage in the power source is sufficiently recovered. Furthermore, the switching process must proceed gradually to avoid possible chattering of the system states due to a sudden change of control forces and therefore a coefficient λ_s, which changes from 0 to1 in a short time, is introduced to the control input when the switch process takes place. The control strategy is summarized in (18).

$$\begin{cases} \boldsymbol{u} = \boldsymbol{K_o x}, \text{ when } W \geq E_{th} \text{ and } \boldsymbol{K_o} \to \boldsymbol{K_o} \\ \boldsymbol{u} = \lambda_s \boldsymbol{K_p x} + (1-\lambda_s)\boldsymbol{K_o x}, \text{ when } W < E_{th} \text{ and } \boldsymbol{K_o} \to \boldsymbol{K_p} \\ \boldsymbol{u} = \boldsymbol{K_p x}, \text{ when } W < E_{th} \text{ and } \boldsymbol{K_p} \to \boldsymbol{K_p} \\ \boldsymbol{u} = \lambda_s \boldsymbol{K_o} x + (1-\lambda_s)\boldsymbol{K_p} x, \text{ when } W \geq E_{th} \text{ and } \boldsymbol{K_p} \to \boldsymbol{K_o} \end{cases} \quad (18)$$

VI. Simulation

Three scenarios are used in the simulation for the validation of the self-powered active suspensions and performance assessment against the passive vehicle. Scenario A represents a condition where the controller is switched between the control gains $\boldsymbol{K_p}$ and $\boldsymbol{K_o}$ (i.e. for a case where a reduction in performance improvement is traded off with the self-powered requirement). In scenario B, the control gain $\boldsymbol{K_o}$ is used and the active suspension provides the best performance improvement under the energy balance condition. In scenario C, the results from the passive vehicle are used for comparisons. $\boldsymbol{K_o}$ is solved by setting $\rho_1=\rho_3=0.01$, $\rho_2=0.4$, $\rho_4=4\times10^{11}$ (designed in Section III) and $\boldsymbol{K_p}$ is that obtained from $\rho_1=\rho_3=0.01$, $\rho_2=0.4$, $\rho_4=1\times10^{-10}$ (which gives a ride quality worse than $\boldsymbol{K_o}$). In the force control loop for the actuators, the proportion gain and the integration gain of the PI controller are set as 6.0 and 0.5, respectively. According to [14], the power loss in the DC/DC and the power source is typically estimated at less than 10% of the overall electric power requirement. So the coefficient μ is set at 15% in this section. The initial energy storage E_{ini} is set as -50J and E_{th} is set as the same as E_{ini}. The computed results of the ride quality indexes and the energy consumption for the track section 1 are shown in TABLE III. Also the energy consumption in time history domain is shown in Fig. 8.

TABLE III
Ride Quality and Energy Consumption for Three Scenarios

Scenario	RMS (mm/s^2)				RMS (mrad/s^2)		Energy
	$\ddot{y}_c$	$\ddot{y}_{c1}$	$\ddot{y}_{c2}$	$\ddot{y}_{cg}$	$\ddot{\psi}_c$	$\ddot{\theta}_c$	(J)
A	16.0	48.4	52.7	39.3	5.3	8.5	-49.9
B	10.5	34.3	38.4	27.7	3.9	5.5	-14.3
C	26.7	75.8	73.3	58.6	7.7	12.7	—

This article has been accepted for publication in a future issue of this journal, but has not been fully edited. Content may change prior to final publication. Citation information: DOI 10.1109/TVT.2015.2407575, IEEE Transactions on Vehicular Technology

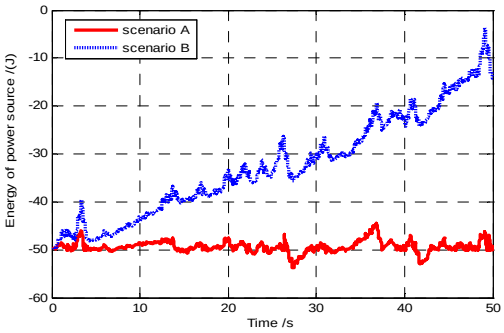

Fig. 8. Energy consumption of the actuators

TABLE III shows that the active suspensions deliver better ride quality in both scenarios than the passive suspension. Scenario B provides the best ride quality in all the 3 scenarios, but with almost more than 2/3 of the initial energy E_{ini} consumed. Moreover, as indicated in Fig. 4, scenario B cannot achieve energy balance if there is an excessive power loss in the power source, i.e. the higher value of μ. In this case, the active control would be switched to use the lower control gains in order to maintain the energy balance. It can be seen from Fig. 8 that the energy consumption in scenario A is kept around the initial energy -50J, confirming that the self-powered condition is achieved by the proposed control strategy. Fig. 9 compares the ride quality (lateral and yaw accelerations) between the 3 scenarios using section 1 of the track data. It is clear that the reduction in performance improvement (in order to maintain the energy balance) for scenario A can be quite small when compared with scenario B and the performance is still better than the passive suspensions.

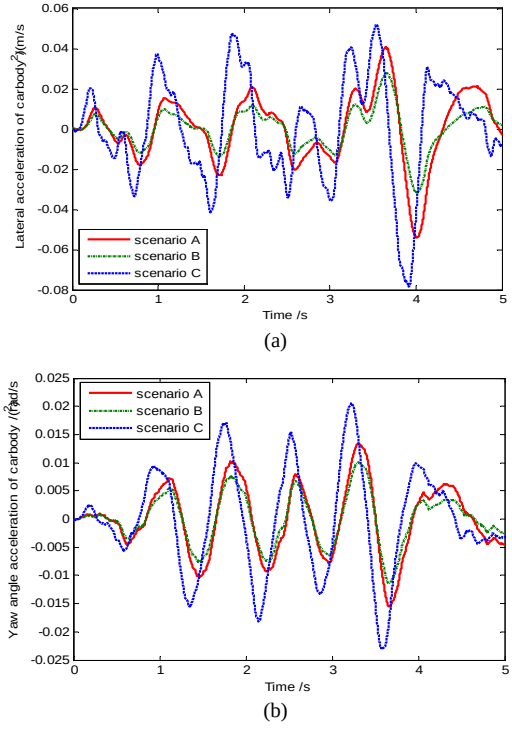

Fig. 9. Indexes of the ride quality of the suspensions (a) $\ddot{y}_c$. (b) $\ddot{\psi}_c$.

TABLE IV shows the ride quality improvements of the active suspensions in comparison to the passive suspensions on all the 3 track sections when applying Scenario A, where the energy consumption is also presented with the same E_{ini} (-50J). It would be noted that the energy balance is guaranteed on every track section and the ride quality improvements are around 30% though there is no external power source to support the actuations.

TABLE IV RIDE QUALITY IMPROVEMENTS AND ENERGY CONSUMPTION

Track No.	RMS improvements (%)						Energy(J)
	$\ddot{y}_c$	$\ddot{y}_{c1}$	$\ddot{y}_{c2}$	$\ddot{y}_{ca}$	$\ddot{\psi}_c$	$\ddot{\theta}_c$	
1	40.1	36.2	28.1	32.9	31.2	33.1	-49.9
2	41.4	38.9	31.3	36.2	34.7	36.8	-59.2
3	28.3	32.8	25.2	29.0	29.0	25.6	-77.5

VII. CONCLUSION

This paper has investigated the development of a self-powered active lateral secondary suspension for railway vehicles. The study has shown that significant energy can be produced from vehicle responses to the track irregularities, which can be used to power the active suspensions without the need for additional power supplies if suitable regeneration measures can be taken. A trade-off analysis between the energy consumption and the ride quality performance has been used to optimize the control design. The analysis of the energy balance condition has indicated that the performance gains in ride quality from the self-powered suspensions are dependent upon the internal power losses of the actuators and the efficiency of the energy recovery/storage - hence the analysis for parameters of the actuator is presented to match the requirement of low internal energy cost. For the less ideal conditions (i.e. with higher power losses and/or changes of the track conditions), a control strategy has been proposed to handle the conditions with the lower level of energy available for harvesting which has been shown to still provide good ride quality improvement while still maintaining the energy balance.

APPENDIX

TABLE V
VARIABLES AND PARAMETERS OF THE VEHICLE

Symbols	Definitions
y_c, y_{t1}, y_{t2}	Lateral displacement of car body, front bogie, rear bogie
$y_{w1}, y_{w2}, y_{w3}, y_{w4}$	Lateral displacement of first wheelset to fourth wheelset
$\psi_c, \psi_{t1}, \psi_{t2}$	Yaw angle of car body, front bogie, rear bogie
$\psi_{w1}, \psi_{w2}, \psi_{w3}, \psi_{w4}$	Yaw angle of first wheelset to fourth wheelset
$\theta_c, \theta_{t1}, \theta_{t2}$	Roll angle of car body, front and rear bogie
$y_{r1}, y_{r2}, y_{r3}, y_{r4}$	Track lateral displacement (irregularities)
U_1, U_2	active force produced by the actuator equipped on front bogie and rear bogie
M_w, M_t, M_c	Wheelset mass (1750kg), bogie mass (3296kg) and car body mass (32000kg)
I_{wz}, I_{tz}, I_{cz}	Wheelset yaw inertia (1400kg · m^2), bogie yaw inertia (2100kg·m^2) and car body yaw inertia (2.24×10^6 kg· m^2)
I_{tx}, I_{cx}	Bogie roll inertia(1900 kg· m^2) and car body roll inertia (75000 kg· m^2)
K_{px}, K_{py}, K_{pz}	Double of primary longitudinal stiffness (2.9×10^{7}N/m), lateral stiffness (1.5×10^{7}N/m) and vertical stiffness (1.33×10^{6}N/m)

This article has been accepted for publication in a future issue of this journal, but has not been fully edited. Content may change prior to final publication. Citation information: DOI 10.1109/TVT.2015.2407575, IEEE Transactions on Vehicular Technology

C_{px}, C_{py}, C_{pz}	Double of primary longitudinal damping (0N·s/m), lateral damping(0N·s/m) and vertical damping (3×10^4N·s /m)
K_{sx}, K_{sy}, K_{sz}	Double of secondary longitudinal stiffness (3.4×10^5N/m), lateral stiffness (3.5×10^5N/m) and vertical stiffness (6.8×10^5N/m)
C_{sx}, C_{sy}, C_{sz}	Double of secondary longitudinal damping (5.0×10^5N·s/m), lateral damping (5.2×10^4 N·s/m) and vertical damping (1.6×10^5N·s /m)
l	Half of bogie center pin spacing (9m)
a	Half of wheelbase (1.25m)
b	Half of wheelset contact distance (0.7465m)
b_1, b_3 , b_2, b_4	Half of primary longitudinal and vertical suspension, and secondary longitudinal and vertical suspension spacing (1m)
h_{cs}	Vertical distance from car body center of gravity to secondary lateral suspension (0.78m)
h_{ts}	Vertical distance from bogie frame center of gravity to secondary lateral suspension (0.22m)
h_{tp}	Vertical distance from bogie frame center of gravity to primary lateral suspension (-0.2085m)
V	Vehicle speed (50m/s)
r_0	Wheel rolling radius (0.4575m)
f_{11}, f_{22}	Longitudinal creep coefficient (1.12×10^7) and lateral creep coefficient (9.98×10^6)
λ	Effective wheel conicity (0.05)

TABLE VI
VARIABLES AND PARAMETERS OF THE ACTUATOR

Symbols	Definitions
x_{act}	Relative displacement of the actuator
x_m	Displacement of the ball-screw
θ_m	Rotation angle of the motor
f_{act}	Force generated by the actuator
v_a , i_a	Voltage and current of the motor
m_{sc}	Screw mass (2kg)
k_{sc}	Screw stiffness (1.8×10^5N/m)
c_{sc}	Screw damping (1.2×10^3Ns/m)
k_m	Motor series stiffness (1×10^7N/m)
c_m	Motor damping (8×10^{-5}N· m· s/rad)
J_m	Motor inertia (3.67×10^{-4}kg· m^2)
n	Screw pitch (7.96×10^{-4}m/rad)
k_t	Motor torque constant (0.297 N· m/A)
k_e	Motor back-emf gain (0.297 V/rad/s)
l_{arm}	Winding inductance (3.7mH)
r_{arm}	Winding resistance (1.8 Ω)

REFERENCES

[1] Y. Suda and T. Shiiba, "A new hybrid suspension system with active control and energy regeneration," *Veh. Syst. Dyn.*, vol. 25, no. S1, pp: 641-654, 1996.

[2] K. Nakano, Y. Suda and S. Nakadai, "Self-powered active vibration control with continuous control input," *JSME Int. J. Ser. C*, vol. 43, no. 3, pp: 726–731, 1999.

[3] K. Nakano and Y. Suda, "Combined type self-powered active vibration control of truck cabins," *Veh. Syst. Dyn.*, vol. 41, no. 6, pp: 449-473, 2004.

[4] K. Nakano, Y. Suda and S. Nakano, "Self-powered active vibration control using single electric actuator," *J. Sound Vib.*, vol. 260, no. 2, pp: 213-235, 2003.

[5] F. Yu, M. Cao and X.C. Zheng, "Research on the feasibility of vehicle active suspension with energy regeneration," *J. Vib Shock*, vol. 24, no. 4, pp: 27-30, 2005.

[6] L. Zuo and P.S. Zhang, "Energy harvesting, ride comfort and road handling of regenerative vehicle suspension," in *Proc. ASME Dyn. Syst. Control Conf.*, Arlington, USA, 2011, pp: 295-302.

[7] Z. J. Li, L. Zuo, L. George, L. J. Lin and Y. X. Qin, "Electromagnetic energy-harvesting shock absorbers design, modeling, and road Tests," *IEEE T. Veh. Technol.*, vol. 62, no. 3, pp: 1065-1074, 2013.

[8] R. Goodall, "Active railway suspensions: implementation status and technological trends," *Veh. Syst. Dyn.*, vol. 28, no.2-3, pp: 87-117, 1997.

[9] S. Bruni, R. Goodall and T.X. Mei, "Control and monitoring for railway vehicle dynamics," *Veh. Syst. Dyn.*, vol. 45, no. 77-8, pp: 743-779, 2007.

[10] O. Anneli, S. Sebasian and P. Rickard, "Ride comfort improvements in a high-speed train with active secondary suspension," *J. Mech. Syst. for Transp. Log.*, vol. 3, no. 1, pp: 206-215, 2010.

[11] O. Anneli, S. Sebasian and P. Richard, "Active lateral secondary suspension with H∞ control to improve ride comfort simulations on a full-scale model," *Veh. Syst. Dyn.*, vol. 49, no. 9, pp: 1409-1422, 2011.

[12] R. H. Zhou, A. Zolotas, R. Goodall, "Integrated tilt with active lateral secondary suspension control for high speed railway vehicles," *Mechatronics*, vol. 21, no. 6, pp: 1108-1122, 2011.

[13] P.Wang, T.X. Mei and J.Y. Zhang, "Towards Self-powered Lateral Active Suspension for Railway Vehicles", in *UKACC 10th Int. Conf. Control*, Loughborough, UK, 2014, pp: 567-572.

[14] A. Pacchioni, R. Goodall and S. Bruni, "Active suspension for a two-axle railway vehicle," *Veh. Syst. Dyn.*, vol. 48, no. S1, pp: 105-120, 2010.

[15] L. H. Zong, X. L. Gong, S. H. Xuan, C. Y. Guo, "Semi-active H∞ control of high-speed railway vehicle suspension with magnetorheological dampers," *Veh. Syst. Dyn.*, vol. 51, no. 5, pp: 600-626, 2013.

Peng Wang received the B.S. and M.S. degree in control theory and control engineering from Southwest Jiaotong University, Sichuan, China, in 2007 and 2010, respectively. He is currently working toward the Ph.D. degree in traffic information and control at Traction Power State Key Laboratory, Southwest Jiaotong University, China.

From 2013 to 2014, he was a Research Assistant with the School of Computing, Science and Engineering, University of Salford, UK. His research interest includes active suspension, energy management for vehicular systems and stability analysis for complex systems.

TX Mei received the B.S. and M.S. degree from Shanghai Tiedao University, Shanghai, China, in 1982 and 1985, respectively, the M.S. degree from Manchester University, Manchester, UK, in 1991, and the Ph.D degree from Loughborough University, Loughborough, UK, in 1994.

He currently holds the position of Chair in Control and Mechatronics at the School of Computing, Science and Engineering, Salford University, Salford, UK. His main research is concerned with railway systems including fault tolerance, condition monitoring and vehicle dynamics.

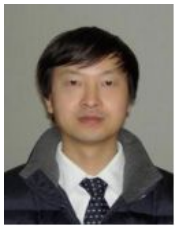

Jiye Zhang received the B.S. degree in mathematics from Chongqing Normal University in 1985, and the M.S. and Ph.D degrees in dynamics and control from Southwest Jiaotong University, China, in 1991 and 1998, respectively.

He is currently a Professor with State Key Laboratory of Traction Power, Southwest Jiaotong University, Chengdu, China. His research interest includes dynamics and control of railway vehicles, and stability analysis and control of complex system.

Hong Li received the B.S. degree from Nanjing University of Aeronautics and Astronautics, Nanjing, China, in1992 and the M. Phil. and Ph.D. degrees from Loughborough University, Loughborough, UK, in 1997 and 2002, respectively.

She is currently a Principal Lecturer with the Department of Engineering and Technology, Manchester Metropolitan University, Manchester, UK. Her research interest includes railway vehicle dynamics, active suspensions, and state estimation.